

# Comparison of Segmentation Methods for Analysis of Endocardial Wall Motion with Real-Time Three-Dimensional Ultrasound

ED Angelini, D Hamming, S Homma, JW Holmes, AF Laine

Department of Biomedical Engineering,  
Columbia University, New York, 10027, USA

## Abstract

*This paper presents a new methodology for validation of endocardial surface segmentation with real-time three-dimensional (RT3D) ultrasound via analysis of ventricular anatomical shape and deformations. When comparing manual tracing and deformable model segmentation methods, we observe high correlation for volume quantification while 3D shapes show significant differences when directly compared by point matching. In the absence of real three-dimensional ground truth for screening of ventricular anatomy, this study aims to define new tests to compare segmented shapes and analyze their accuracy in the context of wall motion analysis.*

*Endocardial surfaces are fitted with finite element modeling in spheroidal prolate coordinates and analysis is performed via construction of node parameter maps in time. Comparison of parameters maps for healthy volunteers and patients with abnormal wall motion are reported.*

## 1. Introduction

Development of three-dimensional ultrasound was initiated in the early 1980s with the introduction of mechanical and freehand transducer probes. In 1990, Von Ramm and Smith introduced a new type of three-dimensional ultrasound system using a matrix phased array that allowed the acquisition of an entire volume in real-time (1). With this real-time three-dimensional (RT3D) ultrasound system, echocardiographic data offers great potential for enhanced diagnosis with faster and more reliable acquisition as the transducer is in a fixed position during the entire screening examination and tomographic reconstruction is not required for volumetric data visualization.

In two previous studies (2, 3) we developed and validated manual tracing and deformable model segmentation methods for quantification of ventricular volume and ejection fraction. In these studies, we considered manual

tracing on MRI data as ground truth. Deformable models showed higher accuracy and reduced variability when compared to manual measurements taken from MRI on the same patients. These studies also showed the superiority of a 3D deformable model over a 2D implementation in further reducing measurement variability.

Here, we are interested in a more complex validation where we can assess the value of our segmentation methods in reconstructing endocardial surfaces for analysis of wall motion. The definition of a ground truth for such application is more complex and a rigorous validation of the method should evaluate accuracy of the segmentation for extraction of anatomical features. Because of the low resolution of RT3D ultrasound data and poor contrast at the myocardial wall interface, cardiologists tended to trace round contours when manually extracting endocardial borders. On the other hand, deformable models will tend to extract curved shapes defined as an equilibrium between internal rigidity forces and external edge-attractor forces. Even though the two methods agree with high correlation for volume quantification, 3D shapes show significant differences when directly compared for point matching. In addition, because of the low resolution at the endocardial wall, it is quite possible that an automated segmentation tool which incorporates 3D or 4D information will perform better than an expert tracing borders on 2D static planar views. The use of a second screening modality for comparison is difficult as typically both spatial and temporal resolutions will differ greatly and affect the level of anatomical details that a specific method (i.e. screening protocol and segmentation method) can achieve.

In the absence of real three-dimensional ground truth for screening of ventricular anatomy, this study aimed to define new tests to compare segmented shapes and analyze their accuracy for wall motion analysis.

In order to reduce the number of parameters, segmented shapes are first fitted with a finite element model in spheroidal prolate coordinates. Modal analysis is then performed via construction of node parameter maps in time. Differences of maps at specific times in the

cardiac cycle are analyzed for a set of landmark locations on the endocardial surface and comparisons are made between the two segmentation methods. Recent efforts from Joshi et al. (4) addressed a similar problem and derived a new shape analysis methodology based on medial representation that can be used for characterization of anatomical objects and applied to quantitative studies of biological variability exhibited by two segmentation methods.

The ultimate goal of this analysis is to evaluate the sensitivity and specificity of the 3D deformable model and manual tracing segmentation methods at isolating wall motion abnormalities using true four-dimensional (3D+Time) echocardiographic signal acquired with RT3D ultrasound.

## 2. Methodology

In this section we describe three steps of segmentation, FEM fitting and wall motion parameterization.

### 2.1. Segmentation of endocardial surfaces

The segmentation methods presented in this work include manual tracing on original RT3D ultrasound data and 2D deformable model segmentation on denoised data as previously presented in (3). Because of the true volumetric nature of RT3D data, it seemed desirable to extend the segmentation process to 3D and fully exploit the spatial continuity of the ultrasound signal in the three dimensions. New 3D deformable models, extensively studied in the recent thesis of Montagnat (5), are still undergoing major adjustment related to modelization and implementation (6). In particular, level set algorithms, recently introduced by Osher and Sethian (7) offer a very simple framework for implementation of deformable surfaces in  $n$ -D. Extensive literature has reported successful implementation of gradient-based level set algorithms for multidimensional segmentation of medical images (8). In this work, we have implemented a 3D segmentation method based on the Mumford-Shah functional within a level set framework as proposed by Chan and Vese in (9).

Endocardial contours produced by the three segmentation methods revealed great variability in smoothness and levels of detail. Manual tracing produced rounder surfaces in short axis cross section while 3D level set produced highly curved contours but ensured smoothness in the long axis dimension. These observations are illustrated in Figure 1 on cross sections for two RT3D exams.

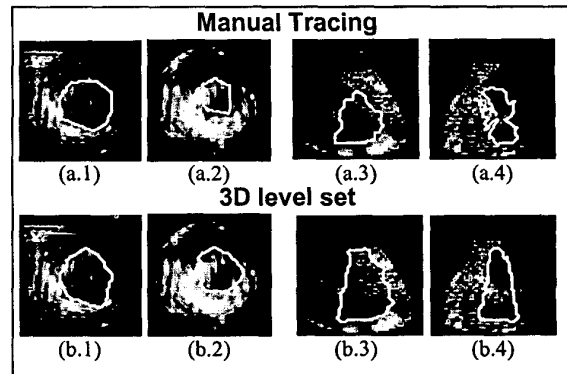


Figure 1. Segmentation of endocardial surfaces. Cross-sectional images and endocardial contours are displayed in short-axis (a1-a2, b1-b2) and long-axis (a3-a4, b3-b4) views. Segmentation methods include (a) manual tracing and (b) 3D deformable model (level set).

### 2.2. FEM fitting

Studies of left ventricular geometry have demonstrated the efficiency of prolate spheroidal coordinate system for modeling of endocardial and epicardial surfaces (10). This coordinate system employs a radial coordinate  $\lambda$  and two angular coordinates  $\mu$  and  $\theta$ , with surfaces of constant  $\lambda$  describing concentric ellipsoids, as illustrated in Figure 2. Segmented data were first transformed to a Cartesian coordinate system centered at a floating centroid position defined for each time frame. Transformation between this Cartesian system and a prolate spheroidal coordinate system centered about the same origin is given by (10).

Endocardial data points were fitted with a 64-element finite element model and cubic Hermite polynomial interpolation (10) using the custom finite element package Continuity 5.0 developed at the University of California San Diego (<http://cmrg.ucsd.edu>). An original undeformed ellipsoid mesh was defined with  $16^\circ < \mu < 120^\circ$  value from base to apex and  $\lambda = 1$ .

Data points were then projected onto the undeformed surface along lines of constant  $\mu$  and  $\theta$  and the fitted surface  $\lambda = \lambda(\mu, \theta)$  determined by least squares minimization of the distance between the data points and their assigned location on the surface, converting the fitting problem to a computationally efficient scaled linear least-squares minimization problem (10). This fitting process is illustrated in Figure 2.

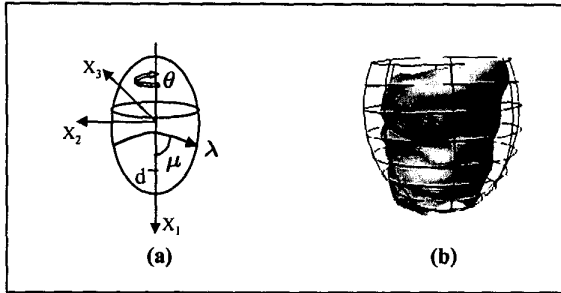


Figure 2. Endocardial surface fitting process with FEM. (a) Prolate spheroidal coordinate system  $(\lambda, \mu, \theta)$  in 3D. (b) Initial FEM mesh and fitted endocardial surface from segmented data using 3D deformable model.

### 2.3. Wall motion parameterization

Each fitted surface  $\lambda = \lambda(\mu, \theta)$  provided a parametric representation of the LV endocardial surface on polynomial basis functions. The collection of multiple fitted surfaces from a series of consecutive time frames constituted a parametric representation of LV endocardial surface motion  $\lambda = \lambda(\mu, \theta, t)$  on a polynomial spatial basis and discrete temporal basis.

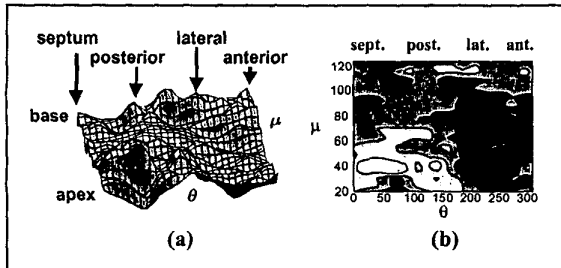


Figure 3. Endocardial surface parameter maps. (a) Fitted endocardial surface unwrapped and projected on a 2D surface  $\lambda = f(\mu, \theta)$ . (b) Contour plot of fitted endocardial surface (a) (lighter color indicates greater value).

As illustrated in Figure 3, endocardial surfaces were exported as iso-contour plots of the fitted parameter  $\lambda = \lambda(\mu, \theta)$  over the parameters range:  $16^\circ < \mu < 120^\circ$  and  $0^\circ < \theta < 315^\circ$ . Contractions between end diastole (ED) and end systole (ES) surfaces were visualized by iso-contour plots of the  $\lambda$  values difference between two fitted surfaces.

## 3. Experiments

The focus of this first study was to define new tests to compare segmented endocardial shapes and analyze their accuracy for wall motion analysis. Based on previous studies of ventricular anatomy and regional wall motion,

we anticipated that both the parameter  $\lambda$  and its change with contraction should be relatively uniform in a correctly segmented dataset.

As our first test we evaluated parametric representations of the endocardial surfaces  $\lambda(\mu, \theta)$  on a normal volunteer to characterize the smoothness of the segmented surface with the three segmentation methods. Parameter maps for the three segmentation methods are displayed in Figure 4.

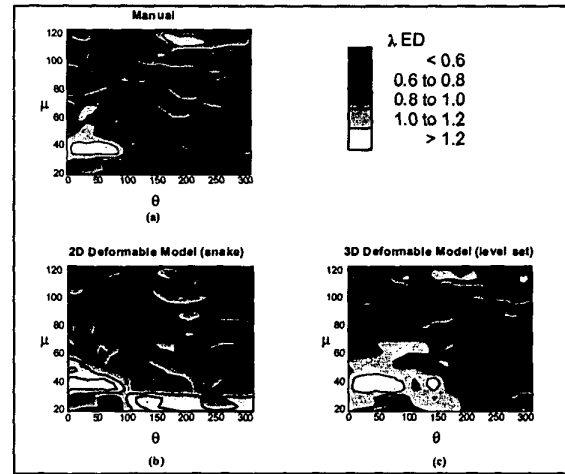


Figure 4: Parameter maps  $\lambda = f(\mu, \theta)$  for the left ventricular endocardial surface of a normal subject at end-diastole with  $0^\circ$  (apex)  $< \mu < 120^\circ$  (base) and  $0^\circ$  (septum)  $< \theta < 270^\circ$  (anterior) walls. (a-c) Iso-contour plots of  $\lambda$  parameter values for each segmentation method.

Visualization of these maps for a normal volunteer at end diastole and end systole showed a relatively large range of variations of the  $\lambda$  parameter across all methods, indicating that uniformity of this parameter is not a useful screen for segmentation errors. However, differences between the maps from different methods did reveal that 2D methods such as manual tracing and 'snakes' performed poorly at defining smooth 3D shapes because of high discontinuities in the third dimension. We also observed that some anatomical features such as invagination of the endocardial wall at location of the papillary muscles were clearly identifiable with each method.

As a second test we looked at contraction maps by subtracting end diastolic and end systolic surface parameter maps as displayed in Figure 5. All three segmentation methods showed relatively uniform contraction over the endocardial surface. A similar test was performed for a patient with a large posterior wall motion abnormality.

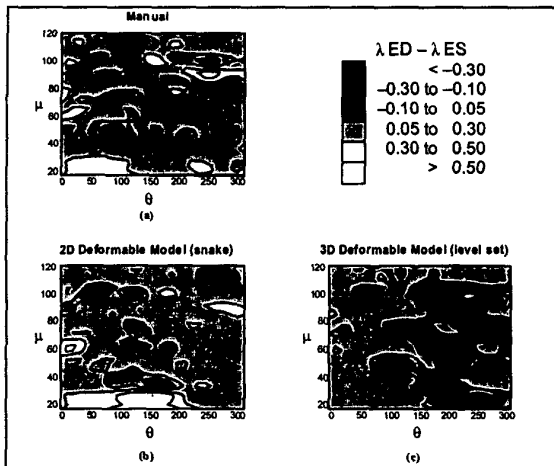


Figure 5: Left ventricular contraction in a normal subject. (a-c) Iso-contour plots of the difference of  $\lambda$  values between end-diastole (ED) surface and end-systole (ES) surface for each segmentation method. Contour levels are spaced to differentiate normal function (0.05 to 0.30) from three levels of dysfunction (darker color) and two levels of hyperfunction (lighter color).

The contraction maps showed much greater variations on overall and clear reduction in motion at the site of the defect. However, the change in  $\lambda$  in the defect region overlapped with values seen in normal subject, indicating too much variability in contraction values to be used for discrimination between normal and abnormal motion.

#### 4. Conclusion

The focus of this study was to compare two state-of-the-art segmentation methods and manual tracing for wall motion analysis using RT3D ultrasound. Such a comparison can be viewed as a qualitative validation of the segmentation methods for a clinical application where the ground truth is not known and is difficult to estimate with objectivity. The three segmentation methods were compared with a normal patient for assessment of endocardial surface contraction. While tracing contours with variable smoothness and locations, the three methods revealed similar endocardial surface geometry and contraction patterns after FEM parameterization suggesting a range of normal variation for the radial parameters at specific times and in contraction between end-diastole and end-systole. However, the radial parameter alone appeared to be insufficient in separating normal from abnormal wall motion, suggesting the need to include temporal information in the fitting process and investigate the parameter's spatial and temporal derivatives. Despite the current limitations, this method shows great promise to assess the performance and clinical significance of segmentation methods applied to

myocardial wall motion analysis.

#### Acknowledgements

The authors would also like to thank Dr. Donis, Dr. Gersony, Dr. Takuma and Dr. Hirata for their assistance in acquiring and manually tracing the RT3D data sets. The authors also thank Volumetrics © and 3D Echotech © for their assistance. This project was partly funded by the American Heart Association grant 0151250T (AFL) and the NSF grant BES-02-01617 (JWH).

#### References

1. Von Ramm OT, Smith SW. Real time volumetric ultrasound imaging system. *Journal of Digital Imaging* 1990;3(4):261-266.
2. Angelini ED, Laine AF, Donis J, Gersony D, Homma S. Quantification of right and left ventricular function with real-time three-dimensional ultrasound. In: 23rd Annual International Conference of the IEEE Engineering in Medicine and Biology Society; 2001 October; Istanbul, Turkey; 2001. p. 2587-2590.
3. Angelini E, Laine A, Takuma S, Holmes J, Homma S. LV volume quantification via spatio-temporal analysis of real-time 3D echocardiography. *IEEE Transactions on Medical Imaging* 2001;20(6):457-469.
4. Joshi S, Pizer S, Fletcher PT, Yushkevich P, Thall A, Marron JS. Multiscale deformable model segmentation and statistical shape analysis using medial descriptions. *IEEE Transactions on Medical Imaging* 2002;21(5):538-550.
5. Montagnat J, Delingette H, Ayache N. A review of deformable surfaces: topology, geometry and deformation. *Image and Vision Computing* 2001;19(14):1023-1040.
6. Frangi AF, Niessen WJ, Viergever MA. Three-dimensional modeling for functional analysis of cardiac images, a review. *IEEE Transactions on Medical Imaging* 2001;20(1):2-25.
7. Osher S, Sethian JA. Fronts propagating with curvature-dependent speed: Algorithms based on Hamilton-Jacobi formulations. *Journal of Computational Physics* 1988;79:12-49.
8. Malladi R, Kimmel R, Adalsteinsson D, Sapiro G, Caselles V, Sethian JA. A geometric approach to segmentation and analysis of 3D medical images. In: *Mathematical Methods in Biomedical Image Analysis*; 1996 June 21th-22th; San Francisco, CA, USA; 1996. p. 244 -252.
9. Chan TF, Vese LA. Active contours without edges. *IEEE Transactions on Image Processing* 2001;10(2):266 - 277.
10. Hunter PJ, Smaill BH. The analysis of cardiac function: a continuum approach. *Progress in Biophysics and Molecular Biology* 1988;52:101-164.

Address for correspondence.

Andrew Laine  
 Department of Biomedical Engineering  
 Columbia University, ET 351, MC 8904  
 1210 Amsterdam Avenue  
 New York, NY 10027  
 USA